The point-spread-function and the spatial resolution of PIV cross-correlation methods

G.E. Elsinga[1], **J. Westerweel**[1]

[1]Laboratory for Aero and Hydrodynamics, Delft University of Technology, Leeghwaterstraat 21, 2628CA Delft,
The Netherlands
g.e.elsinga@tudelft.nl

ABSTRACT

In this paper a simple method is employed to determine the 1D point-spread-function (PSF) of PIV cross-correlation from a single computer generated image containing a step displacement field. The results for an advanced iterative window deformation cross-correlation algorithm indicate that it acts as a linear filter on the actual particle displacement distribution, provided the particle image diameter is large enough and the magnitude of the displacement step is small enough. As demonstrated, the measured distribution can, in that case, be determined by a convolution of the actual particle displacement fields with the obtained PSF. Moreover, the measured field can be de-convoluted yielding a much-improved estimate for the actual particle displacement. Based on the PSF the spatial resolution can be defined, which is shown to be equal to basic single pass correlation at best. This contrasts some earlier statements on the spatial resolution of these advanced algorithms that were based on the frequency response function. Limitations of the latter approach are discussed as well. Furthermore, for a given cross-correlation window size, the PSF is shown to depend on the particle image size, but hardly on the particle image density and the cross-correlation window overlap.

1. INTRODUCTION

In PIV measurements, the flow velocity information in each point is spread out in space mainly due to the use of finite size cross-correlation windows. The contribution of the actual velocity in a particular point to the velocity measurement in its neighbourhood is described by the point-spread-function (PSF). The measurement thus yields a weighted average velocity over the window, which has a filtering effect. Assuming the PIV correlation analysis acts as a linear filter on the actual velocity field, the PSF completely describes the effect of finite spatial resolution, and therefore provides the natural basis for the definition of resolution in the physical space. This is especially true for PIV investigations into the spatial structure of a flow, which has been the main area of application of the technique. Think, for example, of the study of coherent structures in turbulence, where, among other things, the physical dimensions and spacing of these structures are of particular interest.

Interestingly, up to now the spatial resolution of the various PIV cross-correlation algorithms has been defined and compared in Fourier space using a frequency response threshold (e.g. Willert and Gharib 1991, Raffel et al. 2007, Stanislas et al. 2008, Schrijer and Scarano 2008) rather than physical space using the PSF. Apart from the fact that thresholding is arbitrary, the frequency response function definition has another disadvantage in that one cannot tell directly whether two flow structures separated in physical space can actually be distinguished or not. This is an important shortcoming as PIV investigations are more often concerned with physical space rather than Fourier space. In this paper, we show in more detail how this change of perspective leads to different conclusions regarding the spatial resolution.

Moreover, the whole frequency response concept is meaningful only when the cross-correlation analysis acts as a linear filter, which may apply under certain displacement-range restrictions requiring that the variations in particle image displacement remain small (Olsen and Adrian 2001, Westerweel 2008). The displacement range for which linearity factually applies has not yet been established, nor has it been shown what happens if the criterion is violated. Note that this theory is for basic single-pass cross-correlation, the situation for the more advanced iterative multi-grid window deformation cross-correlation algorithms (Scarano 2002) is all together less clear. Nonetheless, linear filter theory has been used with some success to describe the stability of the iterative correlation process (Nogueira et al. 1999, Astarita 2007, Schrijer and Scarano 2008).

The important advantage of a possible linearity of PIV cross-correlation is that elaborate numerical simulations to study the effect of spatial resolution in a particular flow (e.g Worth et al. 2010 for homogeneous isotropic turbulence) are not necessary and the actual velocity distribution may simply be convoluted with the PSF to get the corresponding distribution returned by PIV. The reverse may also be of interest; knowledge of the PSF can be applied to de-convolute a measured velocity distribution as to increase the final spatial resolution (a demonstration will be given in the present paper). This may be of interest as a way to enhance the level of detail very close to a wall in a turbulent boundary layer, where even the average flow changes significantly over a relatively small scale. Furthermore, the PSF or frequency response of the measurement technique is required in methods to correct turbulent dissipation accounting for the un- or poorly resolved scales (Lavoie et al. 2007).

The aim of the present paper is to determine the PSF of the current advanced cross-correlation methods in an easy way using a single computer generated test image (§2) and use it in defining the spatial resolution of PIV more rigorously then before (§5). This will lead to a different conclusion regarding the improvements in resolution achieved by the iterative window deformation algorithm. The current approach allows further checking of the assumed linearity of the advanced cross-correlation and establishing the range of conditions for which it is valid (§3). Within the linear range a de-convolution of the measured velocity distribution may enhance the spatial resolution of the measurement as demonstrated in §4. Even in case of non-linearity, the PSF still provides the actual spreading of velocity information for the specific condition considered, as opposed to the frequency response, but without any general applicability to all other points in the flow. Furthermore, the effects of certain experimental parameters on the PSF can be assessed. Here, we will consider the seeding density, the particle image size (§3) and the window overlap (§5). The low seeding concentration cases affecting the spatial resolution are rarely discussed, but are in fact most relevant to Tomographic-PIV applications, where correlation volumes contain usually only five to ten tracers (Elsinga et al. 2006, Elsinga 2008). Small and large particle image diameters, when measured in pixel units, are typically encountered in high-speed PIV due to a larger pixel pitch on the sensor (Hain et al. 2007) and long-range micro-PIV (Kähler et al. 2006) respectively. The assessment of all three PIV techniques finds renewed interest within the European AFDAR research project (Advanced Flow Diagnostics for Aeronautical Research), which commenced recently in 2010. Presently, we determine only the response to a 1-D velocity signal.

2. METHOD TO DETERMINE THE PSF

In principle the PSF may be determined from existing plots of the frequency response function via a Fourier transform. However, the problem is that these available response functions do not extent beyond $Ws/\lambda = 1$, or up to 4 occasionally, where Ws the linear dimension of the correlation window and λ is the spatial wavelength of the velocity signal. To accurately represent the PSF a much wider range of wavelengths would be needed. It is a direct consequence of the PSF being spatially compact, which means its Fourier transform, i.e. the frequency response, must be broad. If one realizes that each wavelength requires the evaluation of a synthetic PIV image (or alternatively combining these into one single, but very large, image as in the PIV challenge, see Stanislas et al. 2008), it becomes clear than this approach can be rather computationally demanding.

Therefore, we propose to use a simple and direct approach to obtain the 1-D PSF, which is based on the cross-correlation analysis of a computer generated PIV image containing a step change in the particle displacement field (the integral of a pulse). The particle displacement is taken parallel to the step and changes from $-\Delta x$ to $+\Delta x$ across the interface. Furthermore, the y-direction is taken normal to the step. By spatial differentiation of the measured displacement field with respect to y and normalizing it with the step height, the normalized pulse response, or PSF, is obtained. As a result of the normalization, the area under the PSF is equal to one. Only a single image for a given step height and particle imaging conditions would suffice this way. The images used here are 1311x151 pixels in size, where the larger dimension is the homogeneous direction running parallel to the step, over which direction the particle displacement profiles are averaged. The particle images are Gaussian with a peak intensity of 80 counts and a radius r_p, which is defined as $2\sqrt{2}$ times the variance of the Gaussian distribution. Should the frequency response function be required also, it can be computed via a Fourier transform of the PSF.

The approach is illustrated in figure 1 showing the average measured particle displacement profiles for different step heights $2\Delta x$ (left) and the resulting PSFs (right). The cross-correlation algorithm used is an iterative window deformation method (Scarano 2002) with 5 iterations and a second order regression predictor filter between iterations (Schrijer and Scarano 2008). This method will be used throughout this paper unless indicated otherwise. The correlation window size is fixed at 31x31 pixels and the window overlap is 97% as to have a displacement vector at each pixel location. Results for different overlap factors will be discussed at the end of §5, where it will be demonstrated that a reduction in overlap mainly introduces additional discretization effects, rather than causing an important change in the PSF.

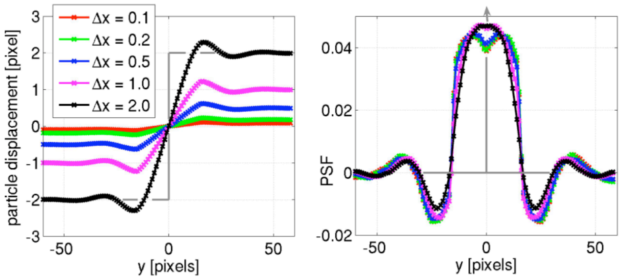

Figure 1. Particle displacement profiles over a step returned by an advanced PIV algorithm (left) and corresponding PSFs (right), which were obtained from the displacement profiles by a spatial differentiation and normalization by the step height $2\Delta x$. The original input step into the PIV recordings for $\Delta x = 2$ pixels (left) and the corresponding pulse (right) are indicated in gray. The particle density was 0.05 particles per pixel and the particle image radius r_p was 1.0 pixel. The y-coordinate represents the distance relative to the step.

3. LINEARITY AND NON-LINEARITY OF THE CROSS-CORRELATION

The PSF shows how much the actual velocity at the pulse location ($y = 0$) contributes to the velocity measurement in its neighbourhood. If the PIV cross-correlation analysis is linear this spreading function should be independent of the magnitude of the particle displacement distribution, that is the step height in the present case.

The results in figure 1-right indicate that for step heights below 1 pixel particle displacement ($\Delta x \leq 0.5$ pixel), the PSF is indeed independent of the step height, which is evidence for linearity of the PIV evaluation in that range. The width of the central peak (-15 to +15 pixels) is equal to the correlation window width. The negative (at 25 pixels from the center) and small positive (around 40 pixels from the center) side lobes clearly show that the particle displacement information is spread beyond a correlation window when using these advanced correlation methods. Increasing the half step height Δx to 1 and 2 pixel seems to yield only a small effect by reshaping the peak around $y = 0$ and increasing the main peak height while decreasing slightly the magnitude of the side lobes.

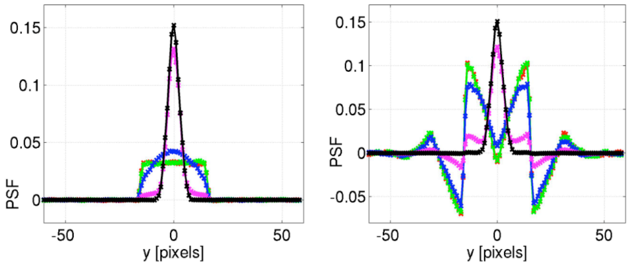

Figure 2. PSFs for single pass (left) and iterative window deformation without predictor filtering, 5 iterations (right). For the legend and particle imaging conditions see figure 1.

For standard single pass cross-correlation a top hat PSF is returned having a width equal to the correlation window, as expected (figure 2-left). Linear behaviour, however, is found over a reduced range up to $\Delta x = 0.2$ pixel. Furthermore, the single pass cross-correlation yields a narrow PSF of only 15 pixels wide for half step heights above $\Delta x = 1.0$ pixel. At that point the correlation peak splits into two; corresponding to the particle displacement on either side of the step. Depending on the position relative to the step one peak will prevail. The transition from the top hat PSF to the narrow peak is rapid. Including the predictor filtering step in the iterative PIV cross-correlation algorithm, however, makes this transition from linear behaviour to non-linearity much more gradual. This can be seen when comparing the results for iterative window deformation with (figure 1-right) and without (figure 2-right) predictor filtering. When filtering is applied the PSF depends less on the step height. So much so that the differences become relatively small (compare the cases $\Delta x = 0.2$ and 1.0 pixel in figure 1-right).

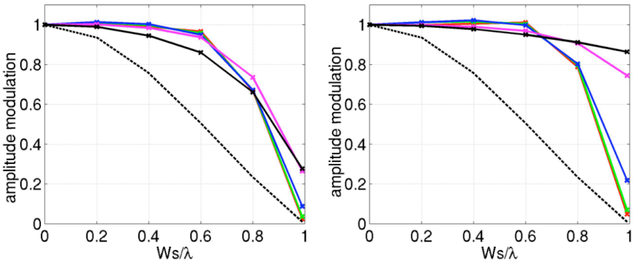

Figure 3. Frequency response for iterative window deformation with (left) and without predictor filtering (right) showing the amplitude modulation versus wavelength λ. These results have been obtained using the PSFs in figure 1-right and figure 2-right respectively. The dashed line indicates the response for a top hat filter.

To illustrate the advantage of the present PSF approach to describe the spatial resolution effects in PIV over earlier frequency response approaches, the latter are presented in figure 3 for the cases with and without predictor filtering. They have been obtained by a Fourier transformation of the corresponding PSFs and match with the plots reported in the literature (e.g. Raffel et al. 2007, Schrijer and Scarano 2008). Apart from some minor differences in the range $0.6 < Ws/\lambda < 0.8$, the frequency response for small steps (i.e. the linear range) is nearly independent of whether or not predictor filtering has been applied, which may wrongfully suggest that the spatial response of the PIV correlation analysis is unaffected. The corresponding PSFs, however, clearly show something very different; compare figure 1-right and figure 2-right. Perhaps the most striking difference is seen near $y = 0$, where the PSF either reaches a maximum (with predictor filtering) or becomes nearly zero (without predictor filtering). The latter means the actual velocity is not contributing to the PIV velocity measurement in the same point, which is undesirable. Such an important change in the behavior of the cross-correlation is not easily picked up from the frequency response.

Furthermore, PSFs were determined for varying particle image radius r_p = [0.5, 1.0, 2.0, 5.0, 10] pixel and image seeding densities expressed in particle per pixel ppp = [0.002, 0.005, 0.010, 0.050, 0.100], which covered the range from an average of 2 particles per correlation window up to 100. The effect of the particle image radius is illustrated in figure 4. For the smallest particle image tested ($r_p = 0.5$ pixel, figure 4-left), no linear behaviour is observed. All step heights result in a different PSF. Hence, for poorly resolved particle images the spatial resolution will depend on the details of the particle image displacement field. In these circumstances the general frequency response functions and the PSFs, as well as a linear theory are meaningless. For particle images that cover multiple pixels ($r_p \geq 1.0$ pixel) linearity does apply provided the step height is below a certain threshold, which increases with particle image size as may be expected (Olsen and Adrian 2001, Keane and Adrian 1992). For $r_p = 1.0$ pixel the PSF does not change up to $\Delta x = 0.5$ pixel (figure 1-right), while for $r_p = 5.0$ pixel this is up to $\Delta x = 1.0$ pixel (figure 4-right). Moreover, the larger particle images tend to smoothen the PSF, which reduces the dip in the peak at $y = 0$ as well as the magnitude of the side lobes (compare figures 1 and 4).

Independence of the PSF on the seeding density was reached for the cases where the source density $Ns = r_p^2 \cdot ppp$ (Adrian 1991) was larger than 0.02. For $r_p = 1.0$ and 2.0 pixel this requirement was met at $ppp = 0.050$ and 0.005 respectively. Note that the results presented in this paper are for $ppp = 0.050$, hence fulfil this condition.

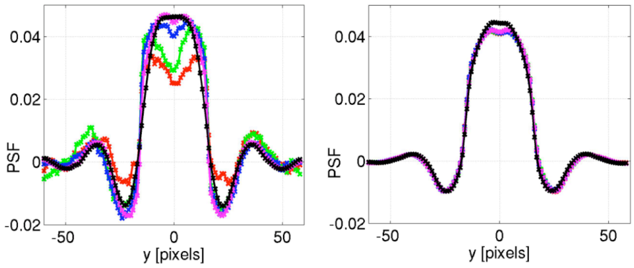

Figure 4. PSFs for different step heights (legend see figure 1) and particle image radii r_p of 0.5 pixel (left) and 5.0 pixels (right). The particle density was 0.05 particles per pixel.

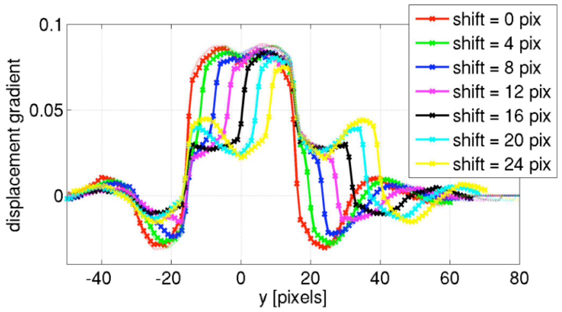

Figure 5. Particle displacement gradient profiles obtained from computer generated images containing two steps shifted with respect to each other by the distance indicated in the legend. The solid lines represent the measured profiles by the cross-correlation analysis and the dashed lines are the profile as predicted by a convolution of the actual displacement field with the PSF of figure 1 ($\Delta x = 0.2$ pixel, $r_p = 1.0$ pixel and 0.05 particles per pixel).

Linearity of the PIV algorithm may additionally be investigated by evaluating a spatially distributed input displacement field in the computer generated PIV recordings. For simplicity, we consider here two 1-D steps of equal height, but shifted in space relative to each other. A spatial differentiation of the average measured particle displacement distribution returned by the PIV algorithm is then presented in figure 5 (solid lines with symbols) for shifts ranging from 0 to 24 pixels in the *y*-direction normal to the step. For comparison the dashed lines show the predicted profiles based on linear theory, which states that these profiles can be obtained by the convolution of the input displacement gradients field (i.e. the two pulses) with the PSF. The PSF for the present imaging conditions was determined beforehand (figure 1). The predicted and measured profile lay almost on top of each other causing the dashed lines to be barely visible. The same level of agreement was found for the full range of shifts considered (up to 40 pixels between the steps, not shown). This further supports the linear model for the advanced PIV algorithm.

4. DECONVOLUTION

The observed linearity of the PIV algorithm can be exploited not only to predict the outcome of a PIV evaluation for a given flow, but also to do the reverse and estimate the actual velocity distribution given the measurement. The latter may be achieved by a de-convolution of the measured displacement field using the known PSF. If successful, this could provide a means to enhance the spatial resolution. The goal here is to demonstrate the possibility rather than making an in depth investigation.

The approach has been tested on the measured profiles of figure 5 using one of the available de-convolution methods included in MatLab. The results are presented in figure 6-left. They clearly reveal peaks at the locations of the pulses that were the input to the original synthetic PIV images, even for small pulse separations. The remaining peak width is only a few pixels, which is close to the actual peak width of one single pixel and constitutes a substantial improvement over the broad distributions in the measured profiles that are on the order of the window size (figure 5). The increase in spatial resolution unfortunately comes at the expense of increased measurement noise. The displacement gradient profiles of figure 6-left are integrated to give the particle displacement distributions (figure 6-right), which clearly reveal the two separate steps. It should be noted that de-convolution may only work for very high overlap and low noise data, but still, the results presented here do suggest the method may hold some potential.

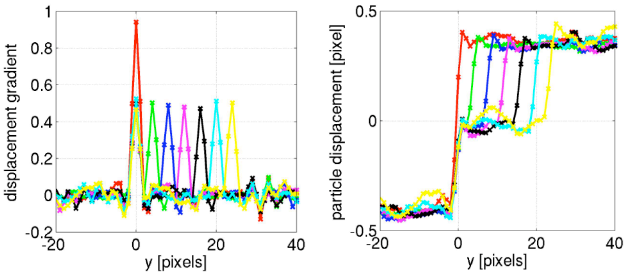

Figure 6. The measured displacement gradient profiles of figure 5 deconvoluted using the PSF (left) with the corresponding particle displacement profile showing the two steps at various separation distances (right). For the legend see figure 5.

5. DEFINITION OF SPATIAL RESOLUTION

With the above PSFs the spatial resolution of a PIV measurement can now be defined. This is useful mostly for the linear regime. But as shown in section 3 the PSFs in the other cases reveal fairly similar characteristics, and therefore, the conclusions reached here are applicable over a much broader range.

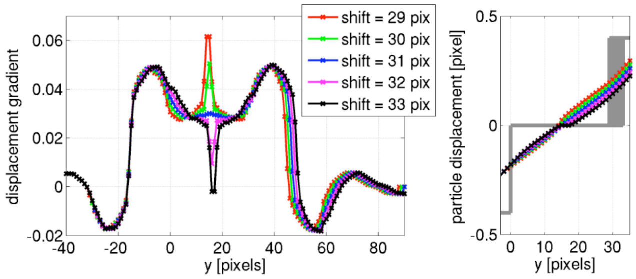

Figure 7. Sum of two PSFs shifted with respect to each other in the *y*-direction (left) showing that the two main lobes separate for shifts exceeding the window size (31 pixels). The integral of the profiles on the left yield the measured particle displacement field (colored lines, right) resulting for an actual displacement field containing two steps (gray lines, right). A plateau becomes visible in these measured profiles for shifts exceeding 31 pixels indicating two separate steps are detectable. The results are obtained using the PSF for the condition $\Delta x = 0.2$ pixel, $r_p = 1.0$ pixel and 0.05 particles per pixel (figure 1).

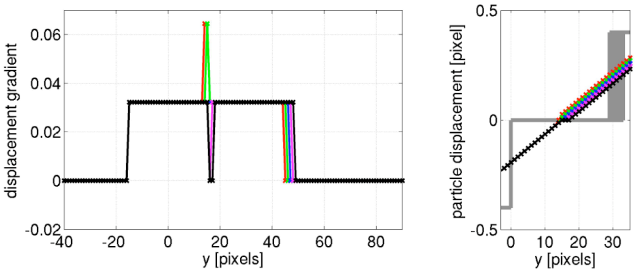

Figure 8. Same as figure 7, but with a top hat PSF representative for a single-pass cross-correlation method using the same window size as in figure 7.

In fact it is possible to come up with two definitions, which differ in strictness. The first, and perhaps more applicable, definition for the spatial resolution is the minimum separation distance at which one can distinguish two features as being different. This is quite similar to its common definition in optics. It can be determined by again taking two equal pulses in the actual particle displacement gradient field and moving them apart until they become visible as two separated pulses in the measured particle displacement gradient. The latter is obtained by a convolution of the actual displacement gradient with the PSF. The result is the superposition of two PSFs, each at the location of a pulse. This approach is illustrated in figures 7-left and 8-left for the advanced PIV algorithm PSF (taken from figure 1) and a top hat PSF representative of a single-pass correlation. Both yield very similar results. For separation distances just below the correlation window size (31 pixels), the two PSF add to produce a high, narrow peak in the middle, which disappears yielding a plateau when the pulse separation is equal to the correlation window size. It is only when the distance between the two PSFs is increased beyond the window size when two distinct main lobes can be identified with a sharp drop in between. Integrating these profiles for two pulses returns the measured particle displacement distribution for two steps (figures 7-right and 8-right). The slope is broken up into two parts when 32 pixels or more separate the steps. Therefore, it is concluded that the spatial resolution of the used advanced PIV algorithm is equal to the cross-correlation window size (plus one pixel), which is exactly the same as for standard single-pass correlation.

The above result is very different from earlier evaluations of the frequency response function, from which it was concluded that the spatial resolution of iterative window deformation is twice better than that of single pass correlation (e.g. Raffel et al. 2007). The frequency response of the more advanced algorithm may indeed be better in certain parts of the spectrum, but the method is unable to perform any better in physically separating two features in the particle displacement field. The latter may appear a detail, but is in fact very important when it comes to the study of coherent flow structures, which are localized events in the velocity field. Their investigation requires detecting and discriminating them in physical space, rather than spectral space, in order to determine their size and spatial organization.

A second, very formal definition of the spatial resolution is the minimum distance over which the measured particle displacements are still strictly uncorrelated. This distance is represented by the width of the PSF based on the points where the tails of the PSF return to zeros. According to this definition, the spatial resolution is about three correlations windows (100 pixels) for the advanced algorithm (figure 1), which is much more than the single window size (31 pixels presently) for a single-pass algorithm.

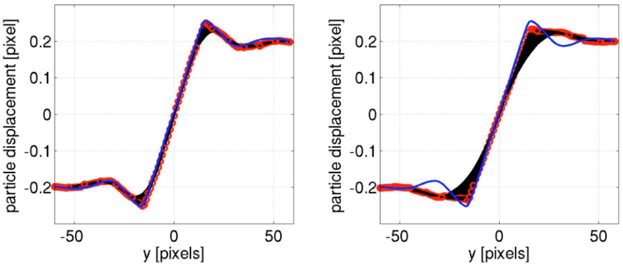

Figure 9. The effect of window overlap on the measured particle displacement across a step. Results are shown for 75% (left) and 50% overlap (right). The same image containing the step was analyzed several times using different measurement grids, which were shifted with respect to each other by one pixel. All profiles thus obtained are shown by the black lines with the individual measurement points marked by the red circles. Combining the points for all grids yield an envelope, which compares well with the profile corresponding to the case where there is a window located at each pixel (97% overlap). This indicated that the PSF of the cross-correlation is unaffected by the overlap and that the overlap only changes the sampling distance.

All results presented thus far have been obtained using a 97% window overlap, which is much higher than found in any experiment. Common overlap factors of 75% and 50% have been considered also, and they yield the same particle displacement profiles across a step (figure 9), hence PSF and spatial resolution. Lower overlap does introduce discretization effects when the undersampling reduces the measured spatial derivatives even further. This can be seen to happen at 50% overlap in the measured particle displacement across a step (the black lines in figure 9-right). Basically, the PSF sets a minimum length scale that can be accessed in the measurement, which depends on the window size. But in order to actually measure that length scale, it should be well sampled on the measurement grid by taking a suitable overlap factor of 75%.

Finally, we consider the effect of smoothing in the vector post-processing step following the PIV cross-correlation analysis. Smoothing is often used to suppress the measurement noise, which is especially critical when it comes to accurately determining velocity gradients (Fouras and Soria 1998, Foucaut and Stanislas 2002). Foucaut and Stanislas consider a smoothing filter to be good, or optimal, when its cutoff wavelength is similar to that of the PIV cross-correlation algorithm. That way noise is reduced without compromising the spatial resolution too much. A second order regression is an example of a filter possessing such properties (Elsinga et al. 2010). Figure 10 shows the effect of this post-processing filter on the final PSF. The width of the main lobe is indeed increased only slightly, while the peak becomes somewhat sharper. The net result is that the spatial resolution as defined above is not really changed.

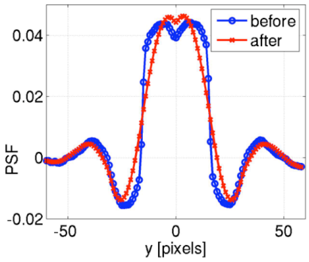

Figure 10. The effect of smoothing in the post-processing of the measured particle displacement field. The profiles show the PSF before and after a second order regression filter has been applied with the kernel size equal to the correlation window size.

6. CONCLUSIONS

The point-spread-function (PSF) was determined for a PIV cross-correlation algorithm with an advanced iterative window deformation method (Scarano 2002). The PSF was obtained by analysing computer generated PIV images containing a step displacement field. The resulting step response was differentiated and normalized yielding the 1-D PSF, which shows how much the actual velocity in a point contributes to the velocity measurement in its neighbourhood.

The PSF of this PIV algorithm resembles a wavelet, where the main lobe width is equal to the cross-correlation window size. The side lobes remain significant over a width covering about three window sizes.

The spatial resolution of the algorithm was defined accordingly as the distance of which separate features in the actual velocity field become distinct in the measurement (one correlation window size), or alternatively the distance of which two measured velocity vectors become completely independent (three correlation window sizes). The latter is clearly a very strict definition. These results show that the spatial resolution of the iterative window deformation methods is, at best, exactly the same as for a basic single pass method.

The above conclusion on the spatial resolution contradicts previous work, in which the spatial resolution has been defined based on the frequency response of the various cross-correlation methods over a limited range of wavelengths. It is true that the advanced iterative deformation method has a better frequency response at intermediate wavelengths, around twice the windows size. However, as shown in this paper this says little about the shape of the PSF, hence on how the actual velocity field is spatially filtered in the measurement. The spatial response issue is important when it comes to one of the prime uses of PIV, that is the investigation of (turbulent) flow structures and determining their exact shape, size and spatial organization. The flow structures that are comparable in size to the correlation window will be affected and it is important to understand how exactly. One effect of the PSF's side lobes is that they may introduce (small amplitude) wiggles in the measured velocity field with a wavelength of around two correlation window sizes, which may potentially result in artificial minima and maxima.

Furthermore, linearity of the correlation method was established provided the particle image diameter is large enough (> 1 pixel) and the change in the particle displacement across the step is below a certain threshold, which increases with particle image size as may be expected. This means the PSF does not depend on the magnitude of the step height in that range and the measured velocity can be obtained from the actual velocity by a convolution with the PSF. Moreover, the measured velocity distribution can be successfully de-convoluted to obtain a better estimate of the actual velocity distribution, provided the measured field has a low noise content. Examples of both convolution and de-convolution were presented in the paper.

The PSF depended on the particle image diameter, but was found to be insensitive to the particle image density and the cross-correlation window overlap factor.

REFERENCES

Adrian R.J. (1991) Particle-imaging techniques for experimental fluid mechanics. *Ann. Rev. Fluid Mech.* **23**: 261-304

Astarita T. (2007) Analysis of weighting windows for image deformation methods in PIV. *Exp. Fluids* **43**, 859-872

Elsinga G.E. (2008) Tomographic particle image velocimetry and its application to turbulent boundary layers. *PhD thesis*, Delft University of Technology, Delft, The Netherlands

Elsinga G.E., Scarano F., Wieneke B. and Van Oudheusden B.W. (2006) Tomographic particle image velocimetry. *Exp. Fluids* **41**: 933-947

Elsinga G.E., Adrian R.J., Van Oudheusden B.W. and Scarano F. (2010) Three-dimensional vortex organization in a high Reynolds number supersonic turbulent boundary layer. *J. Fluid Mech.* **644**, 35-60

Foucaut J.M. and Stanislas M. (2002) Some considerations on the accuracy and frequency response of some derivative filters applied to particle image velocimetry vector fields. *Meas. Sci. Technol.* **13**: 1058-1071

Fouras A. and Soria J. (1998) Accuracy of out-of-plane vorticity measurements derived from in-plane velocity field data. *Exp. Fluids* **25**: 409-430

Hain R., Kähler C. and Tropea C. (2007) Comparison of CCD, CMOS and intensified cameras. *Exp. Fluids* **42**, 403-411

Kähler C.J., Scholz U. and Ortmanns J. (2006) Wall-shear-stress and near-wall turbulence measurements up to single pixel resolution by means of long-distance micro-PIV. *Exp. Fluids* **41**, 327-341

Keane R.D. and Adrian R.J. (1992) Theory of cross-correlation analysis of PIV images. *Appl. Sci. Res.* **49**, 191-215

Lavoie P., Avallone G., De Gregorio F., Romano G.P. and Antonia R.A. (2007) Spatial resolution of PIV for the measurement of turbulence. *Exp. Fluids* **43**, 39-51

Nogueira J., Lecuona P.A. and Rodriguez P.A. (1999) Local field correction PIV: on the increase of accuracy of digital PIV systems. *Exp. Fluids* **27**, 107-116

Olsen M.G. and Adrian R.J. (2001) Measurement volume defined by peak-finding algorithms in cross-correlation particle image velocimetry. *Meas. Sci. Technol.* **12**, N14-N16

Raffel M., Willert C.E., Wereley S.T. and Kompenhans J. (2007) *Particle image velocimetry: A practical guide.* Springer Verlag, Berlin, Heidelberg

Scarano F. (2002) Iterative image deformation methods in PIV. *Meas. Sci. Technol.* **13**, R1–R19

Scarano F. and Riethmuller M.L. (2000) Advances in iterative multigrid PIV image processing. *Exp. Fluids* **Suppl**, S51-S60

Schrijer F.F.J. and Scarano F. (2008) Effect of predictor-corrector filtering on the stability and spatial resolution of iterative PIV interrogation. *Exp. Fluids* **45**, 927-941

Stanislas M., Okamoto K., Kähler C.J., Westerweel J. and Scarano F. (2008) Main results of the third international PIV Challenge. *Exp. Fluids* **45**, 27-71

Westerweel J. (2008) On velocity gradients in PIV interrogation. *Exp. Fluids* **44**, 831-842

Willert C.E. and Gharib M. (1991) Digital particle image velocimetry. *Exp. Fluids* **10**, 181-193

Worth N.A., Nickels T.B. and Swaminathan N. (2010) A tomographic PIV resolution study based on homogeneous isotropic turbulence DNS data. *Exp. Fluids* **49**, 637-656